

¹Johns Hopkins University School of Medicine, Baltimore, MD, USA; ²JHU/APL, Laurel, MD, USA; ³University at Albany, SUNY, Albany, NY, USA; ⁴UCLA, Los Angeles, CA, USA

During spatial navigation, the frequency and timing of spikes from spatial neurons including place cells in hippocampus and grid cells in medial entorhinal cortex are temporally organized by continuous theta oscillations (5–12 Hz). The theta rhythm is regulated by subcortical structures including the medial septum, but it is unclear how spatial information from place cells may reciprocally organize subcortical theta-rhythmic activity. Here we recorded single-unit spiking from a constellation of subcortical and hippocampal sites to study spatial modulation of rhythmic spike timing in rats freely exploring an open environment. Our analysis revealed a novel class of neurons that we termed ‘phaser cells,’ characterized by a symmetric coupling between firing rate and spike theta-phase. Phaser cells encoded space by assigning distinct phases to allocentric isocontour levels of each cell’s spatial firing pattern. In our dataset, phaser cells were predominantly located in the lateral septum, but also the hippocampus, anteroventral thalamus, lateral hypothalamus, and nucleus accumbens. Unlike the unidirectional late-to-early phase precession of place cells, bidirectional phase modulation acted to return phaser cells to the same theta-phase along a given spatial isocontour, including cells that characteristically shifted to later phases at higher firing rates. Our dynamical models of intrinsic theta-bursting neurons demonstrated that experience-independent temporal coding mechanisms can qualitatively explain (1) the spatial rate-phase relationships of phaser cells and (2) the observed temporal segregation of phaser cells according to phase-shift direction. In open-field phaser cell simulations, competitive learning embedded phase-code entrainment maps into the weights of downstream targets, including path integration networks. Bayesian phase decoding revealed error correction capable of resetting path integration at subsecond timescales. Our findings suggest that phaser cells may instantiate a subcortical theta-rhythmic loop of spatial feedback. We outline a framework in which location-dependent synchrony reconciles internal idiothetic processes with the allothetic reference points of sensory experience.

Symmetric & bidirectional phase modulation

Burst theta phase

Mean firing rate (spikes/s)

Phase advance

Phase delay

Integration delay

Spikes

Bursts (ordered)

Thesis: Phaser cells encode allocentric spatial isocontours

Mean theta phase

Negative correlation

Mean firing rate

Positive correlation

Figure 1 displays the results of the proposed method, comparing the performance of the Ring network, Phase slice 1, Phase slice 2, and the All method across different metrics.

The figure is divided into two main sections:

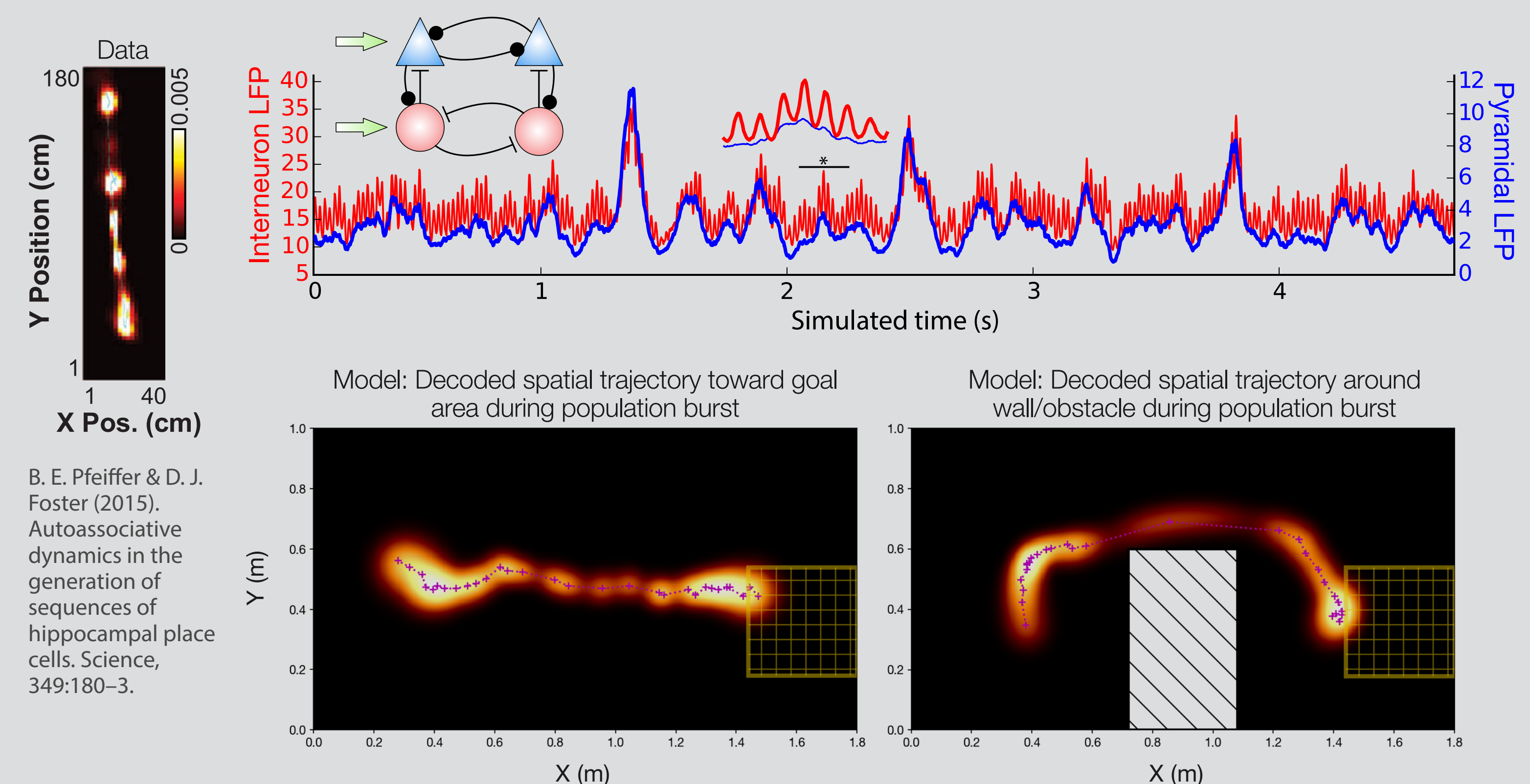
- Left Section: Phase Maps and Trajectories**
 - Ring 'network':** Shows a grid of phase maps (top) and a circular phase map with an actual trajectory (blue line) and MAP estimates (pink line) (bottom).
 - Phase 'slice' 1:** Shows a grid of phase maps (top) and a circular phase map with an actual trajectory (blue line) and MAP estimates (pink line) (bottom).
 - Phase 'slice' 2:** Shows a grid of phase maps (top) and a circular phase map with an actual trajectory (blue line) and MAP estimates (pink line) (bottom).
- Right Section: Performance Metrics**
 - Top Plot: Normalized MSE vs Time lag (s)**

This plot shows the Normalized Mean Squared Error (MSE) as a function of time lag (s) for the Ring, Phase 1, Phase 2, and All methods. The Ring method shows the highest MSE, while the Phase 1 and Phase 2 methods show significantly lower MSE, indicating better performance in estimating the phase maps.
 - Bottom Plot: Error-correction time (s)**

This plot shows the error-correction time (s) for the Ring, Phase 1, Phase 2, and All methods. The Ring method has the highest error-correction time, while the Phase 1 and Phase 2 methods have significantly lower error-correction times, indicating faster convergence to the correct phase map.

J. D. Monaco, R. M. De Guzman, H. T. Blair, and K. Zhang (2019). Spatial synchronization codes from coupled rate-phase neurons. *PLoS Comput Biol*, 15(1):e1006741. <https://doi.org/10.1371/journal.pcbi.1006741>

To study trajectory sequences that ‘hover’ at discrete location during peaks in the slow-gamma rhythm (Pfeiffer & Foster, 2015), we have developed a CA3-like recurrent excitatory/inhibitory network model of quadratic ‘place cells’ that produces sharp wave-like population bursts and gamma oscillations. The activity during the population bursts can be decoded into allowable spatial trajectories that find goals and avoid obstacles.



A Rat 6, tt7_c1 [97]

B Mean firing rate

C Mean spike phase

D Low rate
High rate

E

F Resultant vector of spike phase

20 cm

Lag (ms)

Spike θ -phase

300 ms

Spikes — LFP θ -waves

Burst phase

Mean firing rate (spikes/s)

Mean spike phase

Mean firing rate (spikes/s)

Negative vs. positive phaser cell theta-phase segregation

Phase regression

Recording count

Minimum Peak

Normalized firing rate

Spatial average of mean-phase maps

Negative

Positive

Hippocampal vs. subcortical spike-trajectory mutual information

Spatial rate information (bits/spike)

Directional information (bits/spike)

Speed information (bits/spike)

I_{phase} (bits)

Spatial phase information

Legend:

- ★ Negative (hipp.)
- Negative (not hipp.)
- × Negative (n.s.)
- ★ Positive (hipp.)
- Positive (not hipp.)
- × Positive (n.s.)

Recording Area	Negative	Positive	Mixed	None	Total
Lateral septum	31 (9.7%)	17 (5.3%)	2 (0.6%)	287 (84.4%)	321
Medial septum	–	–	–	16 (100.0%)	16
Hippocampus	11 (12.4%)	4 (4.5%)	–	74 (83.1%)	89
Thalamus	1 (2.2%)	–	–	45 (97.8%)	46
Midbrain	1 (0.7%)	–	–	134 (99.3%)	135
Other	1 (1.6%)	–	1 (1.6%)	62 (96.8%)	64
Total	45 (6.7%)	21 (3.1%)	3 (0.4%)	602 (89.7%)	671

Columns: 'Negative'/'Positive', cells with at least one negative/positive phaser-classified recording and none of the other subtype; 'Mixed', cells with at least one negative and at least one positive phaser-classified recording; 'None', cells with no phaser-classified recordings.

